

Side population in MDA-MB-231 human breast cancer cells exhibits cancer stem cell-like properties without higher bone-metastatic potential

TORU HIRAGA¹, SUSUMU ITO² and HIROAKI NAKAMURA¹

¹Department of Histology and Cell Biology, Matsumoto Dental University, 1780 Gobara-Hirooka, Shiojiri, Nagano 399-0781; ²Division of Instrumental Analysis, Research Center for Human and Environmental Sciences, Shinshu University, 3-1-1 Asahi, Matsumoto, Nagano 390-8621, Japan

Received August 5, 2010; Accepted September 21, 2010

DOI: 10.3892/or_00001073

Abstract. An increasing body of evidence suggests that cancers contain a small subset of their own stem-like cells called cancer stem cells (CSCs), which play critical roles in the initiation, maintenance and relapse of tumors. However, the role of CSCs in cancer metastasis, especially in metastasis to bone, has not been extensively studied. Side population (SP) has been shown to enrich CSCs in several types of cancer, including breast cancer. In the present study, we characterized the SP cells isolated from the human breast cancer cell line MDA-MB-231 in comparison to non-SP (NSP). Fluorescence-activated cell sorter analysis demonstrated the existence of SP in MDA-MB-231 cells, which was markedly reduced in the presence of fumitremorgin C, a specific inhibitor of ATP-binding cassette sub-family G member 2 (ABCG2). Quantitative RT-PCR analysis showed that ABCG2 mRNA expression was significantly higher in SP cells than in NSP cells. SP cells formed increased numbers of tumor-spheres in suspension culture. Furthermore, the tumor growth in the orthotopic mammary fat pad in nude mice was significantly accelerated in SP cells. On the other hand, the development of bone metastases determined by intracardiac injection into nude mice showed no difference between SP and NSP cells. SP abundance in the tumor cells isolated from the bone metastases was not increased either compared with that from the mammary tumors. These results suggest that the SP in MDA-MB-231 cells possesses some of the CSC-like properties but does not have higher metastatic potential to bone.

Introduction

Despite the monoclonal origins, cancers are composed of a heterogeneous population of cells with different properties. It has recently been suggested that, within a given tumor, there exists a small population of cells with the capacity to behave like stem cells called cancer stem cells (CSCs) (1). This concept, which was first established in hematological malignancies (2), has been adapted for a growing number of solid tumors, including breast cancer (1,3). CSCs are characterized by extensive self-renewal and proliferative capacity and resistance to chemotherapy and radiotherapy (1). These characteristic features play pivotal roles in the initiation, maintenance and relapse of tumors. Thus, CSCs are emerging as an important target for cancer therapy.

For identification and isolation of CSCs, several approaches have been proposed. In breast cancers, cell surface markers, such as CD24 and CD44, have been proved to be useful for the isolation of subsets enriched for breast CSCs (1,3). High aldehyde dehydrogenase (ALDH) activity was also recently shown to identify the CSC fraction in breast cancer cells (4). An alternative approach is the side population (SP) phenomenon (5). Owing to the ability to exclude the DNA binding dye Hoechst 33342, SP cells are identified as a tail of dimly stained cells in dual wavelength fluorescent-activated cell sorter (FACS) analysis. Since the original discovery that SP cells in mouse bone marrow are highly enriched for long-term repopulating cells (6), SP cells have been identified in a variety of normal tissues and cancers, including breast cancer and shown to have stem cell-like properties (5,7).

Bone is one of the most preferential metastatic target sites for breast cancer (8). It has been recently suggested that CSCs play an important role in mediating the metastasis of breast cancer (9,10). However, it has yet to be elucidated whether CSCs contribute to the development of bone metastases.

In this study, we identified SP in the human breast cancer cell line MDA-MB-231 and characterized the SP cells as potential CSC-like cells. By taking advantage of the bone metastatic potential of MDA-MB-231 cells in a nude mouse model (11), we examined the ability of SP cells to metastasize to bone.

Correspondence to: Dr Toru Hiraga, Department of Histology and Cell Biology, Matsumoto Dental University, 1780 Gobara-Hirooka, Shiojiri, Nagano 399-0781, Japan
E-mail: hiraga@po.mdu.ac.jp

Key words: side population, cancer stem cell, breast cancer, bone metastasis

Materials and methods

Reagents. Hoechst 33342, fumitremorgin C (FTC), verapamil and doxorubicin were purchased from Sigma-Aldrich (St. Louis, MO). B27 supplement, recombinant human fibroblast growth factor-2 (rhFGF-2) and recombinant human epidermal growth factor (rhEGF) were from Life Technologies Japan, Ltd. (Tokyo, Japan), BioVision, Inc. (Mountain View, CA), and R&D Systems, Inc. (Minneapolis, MN), respectively. 5-Fluorouracil (5-FU) was from Kyowa Hakko Kirin Co., Ltd. (Tokyo, Japan). Matrigel (BD Matrigel Basement Membrane Matrix) was from Becton-Dickinson and Co. (Tokyo, Japan). All other chemicals used in this study were purchased from Sigma-Aldrich or Wako Pure Chemical Industries, Ltd. (Osaka, Japan) unless otherwise described.

Cell culture. Human breast cancer cell line MDA-MB-231 (American Type Culture Collection, Rockville, MD) was cultured in Dulbecco's modified Eagle's medium (DMEM; Life Technologies Japan, Ltd.) supplemented with 10% fetal bovine serum (FBS; Life Technologies Japan, Ltd.) and 100 $\mu\text{g/ml}$ kanamycin sulfate (Meiji Seika Kaisha, Ltd., Tokyo, Japan). In some experiments, MDA-MB-231 cells were cultured in the presence of doxorubicin (10 or 30 nM) or 5-FU (3, 5 or 10 $\mu\text{g/ml}$) for 60 days and the surviving cells were used as doxorubicin- and 5-FU-resistant cells, respectively. The cells were maintained in a humidified atmosphere of 5% CO_2 in air.

FACS analysis and cell sorting. SP analysis and sorting: The protocol was based on Goodell *et al.* (6) with slight modifications. Briefly, MDA-MB-231 cells (1×10^6 cells/ml) were incubated in Hanks' Balanced Salt Solutions (HBSS) supplemented with 2% FBS, 10 mM HEPES, 1% penicillin/streptomycin and 5 $\mu\text{g/ml}$ Hoechst 33342 for 60 min at 37°C with intermittent mixing. In some experiments, cells were incubated with the Hoechst dye in the presence of 2 μM FTC or 50 μM verapamil. After incubation, cells were washed with cold medium and resuspended at 2×10^6 cells/ml, and propidium iodide was added to a final concentration of 2 $\mu\text{g/ml}$ to discriminate dead cells. The gating of SP was based on negative controls in which FTC was used.

SP analysis of tumors from mice: MDA-MB-231 cells were inoculated into the mammary fat pad (5 million cells/0.1 ml PBS) or the left cardiac ventricle (0.1 million cells/0.1 ml PBS) of athymic nude mice (female, 4-week-old, Japan SLC, Inc., Shizuoka, Japan) under anesthesia with pentobarbital (0.05 mg/g body weight; Dainippon Sumitomo Pharma Co., Ltd., Osaka, Japan) (11). Four weeks after the inoculation, mammary tumors and bone metastases were dissected, minced with scalpels and strained through stainless steel mesh. The cells suspended with the culture medium were plated in 10 cm dishes and cultured overnight to remove dead cells and cell debris. Then, SP analysis was performed as described above.

CD24 and CD44 immunostaining: MDA-MB-231 cells were stained with rat monoclonal antibodies against CD24 (FITC-conjugated) and CD44 (PE-conjugated) or isotype-matched IgG controls (all from eBiosciences, Inc., San Diego, CA).

Aldehyde dehydrogenase (ALDH) activity: ALDH enzymatic activity of MDA-MB-231 cells was examined using AldeFluor Kit (StemCell Technologies, Durham, NC) according to the manufacturer's protocol.

All FACS analysis and cell sorting were performed using a BD FACSVantage SE cell sorter (Becton-Dickinson and Co.). The data were analyzed by BD CellQuest Pro software (Becton-Dickinson and Co.).

Cell proliferation in monolayer. SP and NSP of MDA-MB-231 cells (1,000 cells/well/96-well plate) were plated in DMEM supplemented with 10% FBS and 100 $\mu\text{g/ml}$ kanamycin sulfate and cultured for 24, 72 and 96 h. At the end of the culture, the cell proliferation was determined using Cell Proliferation Reagent WST-1 (Roche Diagnostics K.K., Tokyo, Japan) according to the manufacturer's protocol. The absorbance was measured using a microplate reader (Nippon Bio-Rad Laboratories, Tokyo, Japan) at a wavelength of 450 nm.

Tumor-sphere formation. Tumor-sphere formation assay was performed as described previously with some modifications (12). SP and NSP isolated from MDA-MB-231 cells were plated in ultra-low attachment 6-well plates (Corning Japan K.K., Tokyo, Japan) at a density of 2,000 cells/well and cultured in DMEM/F12 (Sigma-Aldrich) containing 2% B27 supplement, 40 ng/ml rhFGF-2 and 20 ng/ml rhEGF for 10 days. The cells were replenished with fresh proliferation medium every 3 days. At the end of the culture, the number of tumorspheres of $>100 \mu\text{m}$ in diameter was counted under a microscope and expressed as the number of tumor-spheres/well.

Quantitative real-time reverse transcriptase-polymerase chain reaction (qRT-PCR). Total RNA was isolated using RNeasy Plus Micro Kit (Qiagen K.K., Tokyo, Japan). Reverse transcription and real-time PCR was performed using One Step SYBR PrimeScript Plus RT-PCR Kit (Takara Bio Inc., Shiga, Japan) in DNA Engine Opticon system (Bio-Rad Laboratories, K.K., Tokyo, Japan) according to the manufacturer's protocol. Primer sequences were as follows: ATP-binding cassette transporters sub-family G member 2 (ABCG2), TGGCTTAGACTCAAGCACAGC/TCGTCC CTGCTTAGACATCC; ABCB1, ACAGAAAGCGAAGCA GTGGT/ATGGTGGTCCGACCTTTTC; glyceraldehyde-3-phosphate dehydrogenase (GAPDH), AGCCACATCGCTC AGACAC/GCCCAATACGACCAAATCC. Melting curve analysis was performed to determine the melting temperature of the amplified product and to exclude undesired primer dimers. Each sample was run at least in triplicate. Quantification was normalized using GAPDH as a reference gene. Expression levels of the particular genes were indicated as fold increase compared with the control.

Microarray analysis. Total RNA was extracted from SP and NSP cells using RNeasy Plus Micro Kit. The RNAs were subjected to microarray full service (Biomatrix Research, Inc., Chiba, Japan) and assessed using GeneChip Human Gene 1.0 ST Array (Affymetrix, Inc., Santa Clara, CA). Array image was scanned and analyzed with GeneChip operating

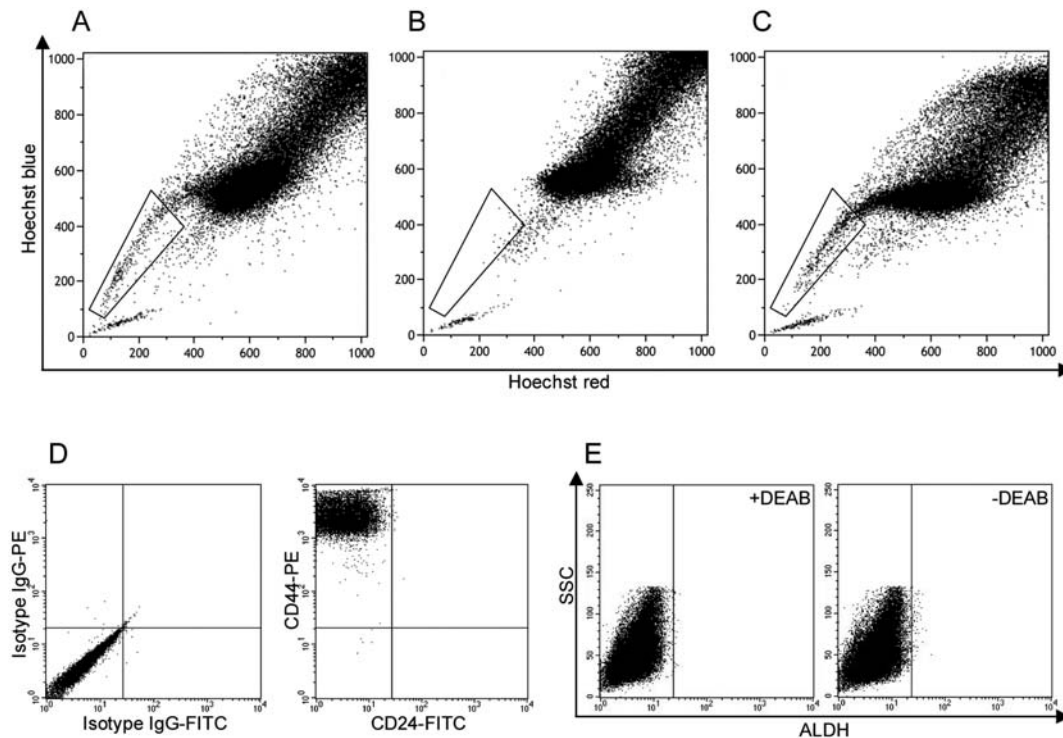


Figure 1. Expression of potential CSC markers in MDA-MB-231 human breast cancer cells. (A-C) Representative Hoechst 33342 dye staining profile in the absence (A) or presence of FTC (B) or verapamil (C). SPs are outlined. (D) CD24 and CD44 expression in MDA-MB-231 cells. The cells stained with isotype control IgGs are shown on the left. (E) ALDH activity of MDA-MB-231 cells in the presence (left) or absence (right) of diethylaminobenzaldehyde (DEAB), an inhibitor of ALDH.

software (Affymetrix, Inc.). Data mining was conducted using GeneSpring software (Agilent Technologies, Inc., Santa Clara, CA).

Animal experiments. Tumorigenesis in mammary fat pad: Under anesthesia with pentobarbital, SP and NSP cells (1,000 or 3,000 cells/0.1 ml matrigel) were injected into the mammary fat pad of athymic nude mice (female, 4-week-old, Japan SLC, Inc.). The size of orthotopic tumors was measured once a week using a caliper. The tumor volume was estimated by the following equation: tumor volume (mm³) = (length) x (width)² x 0.5.

Bone metastasis: SP and NSP cells (10,000 cells/0.1 ml PBS) were injected into the left cardiac ventricle of athymic nude mice (female, 4-week-old, Japan SLC, Inc.) under anesthesia with pentobarbital as described previously (11).

The number of mice used in each experiment is described in each figure. All animal experiments were reviewed and approved by the Animal Management Committee of Matsumoto Dental University.

X-ray analysis. Number and area of osteolytic lesions in the femora and tibiae were determined on radiographs as described previously (11). Data are shown as number of metastases/mouse or lesion area (mm²)/mouse.

Statistical analysis. Data are expressed as the mean \pm SEM. The data were analyzed by one-way ANOVA followed by Fisher's PLSD post-hoc test (StatView; SAS Institute, Inc., Cary, NC) for determination of differences between groups. Student's t-test or Welch's t-test was conducted when two

groups were compared. P-values of <0.05 were considered significant.

Results

Expression of CSC markers in MDA-MB-231 human breast cancer cells. FACS analysis demonstrated that MDA-MB-231 cells after Hoechst 33342 staining were clearly separated into a fluorescence-negative tail of SP (3.40 \pm 0.60%, average of 10 independent experiments) and the brightly stained NSP (Fig. 1A). We also examined other potential CSC markers, CD24/CD44 expression and ALDH activity, in MDA-MB-231 cells. Most of the cells were CD24⁻/CD44⁺ (Fig. 1D) and only a small number of the cells showed ALDH activity (Fig. 1E). Therefore, in the following experiments, we studied the SP of MDA-MB-231 cells as potential CSC-like cells in comparison to the NSP cells.

Characterization of SP cells in vitro. To examine the repopulation ability of the SP of MDA-MB-231 cells, SP and NSP cells were cultured for 2 weeks after cell sorting. Then, the cells were restained with Hoechst 33342 and reanalyzed by FACS. SP cells generated both SP and NSP with fraction size larger than or comparable to the original population (Fig. 2). The SP fraction generated from NSP was smaller than that from SP (Fig. 2).

ABC transporters, especially ABCG2, also known as breast cancer resistance protein (BCRP), and ABCB1, also known as multidrug resistance protein 1 (MDR1), have been implicated as being responsible for the SP phenotype (13,14). Consistent with this notion, quantitative RT-PCR analysis showed that

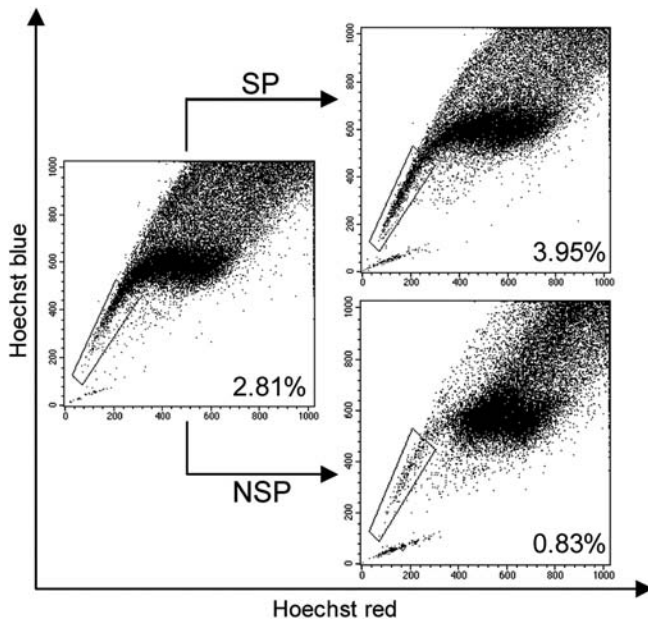


Figure 2. Repopulation ability of the SP of MDA-MB-231 cells. SP and NSP sorted from MDA-MB-231 cells were cultured for 2 weeks. Then, the cells were restained with Hoechst dye and reanalyzed (right figures). Percentages given in the lower right corner refer to the relative abundance of SP cells.

ABCG2 mRNA expression was significantly higher in SP cells than in NSP cells (Fig. 3A), while ABCB1 mRNA was undetectable in both types. Furthermore, the SP fraction was markedly decreased in the presence of FTC, a specific inhibitor of ABCG2 (15), but not in the presence of verapamil, an inhibitor of ABCB1 (16) (Fig. 1B, C).

It has been reported that ABC transporters are involved in drug resistance in cancer cells (17). To determine the relationship between the SP phenotype and drug resistance, we tested the expression of ABC transporters and the SP abundance using MDA-MB-231 cells resistant to doxorubicin and 5-FU, the chemotherapeutic agents widely used for the treatment of breast cancer. ABCG2 mRNA expression was significantly up-regulated in the doxorubicin-resistant cells in a dose-

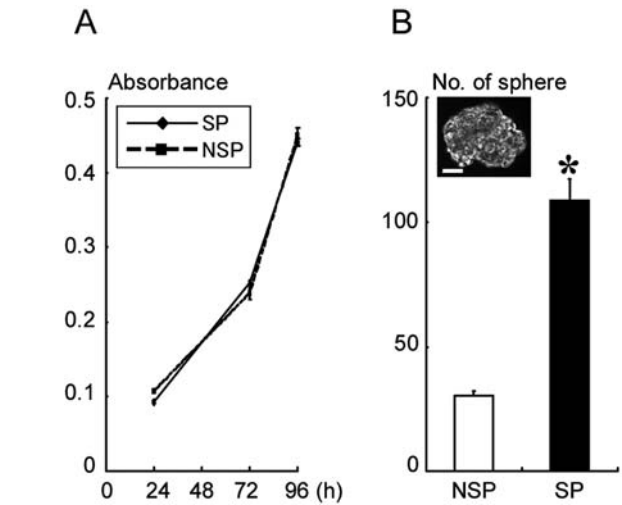


Figure 4. Cell proliferations of the SP of MDA-MB-231 cells *in vitro*. (A) Monolayer cell proliferation of SP and NSP cells determined by WST-1 assay. Data are shown as absorbance at 450 nm. (B) Tumorsphere formation of SP and NSP cells in suspension culture. Data are shown as the number of tumorspheres per well. *Significantly different from NSP ($p < 0.05$). Inset, representative phase contrast image of a tumorsphere formed by SP cells (scale bar, 50 μm).

dependent manner (Fig. 3B), whereas ABCB1 mRNA was not detected in any of the drug-resistant cells. Furthermore, the SP abundance was increased in the doxorubicin-resistant cells (Fig. 3C). These changes were not observed in the 5-FU-resistant cells (data not shown).

We then examined the cell proliferation of SP *in vitro*. Monolayer cell proliferation of SP cells was similar to that of NSP cells (Fig. 4A). In contrast, the tumorsphere formation in suspension culture was significantly enhanced in SP cells (Fig. 4B).

Tumorigenic and metastatic potential of SP cells in nude mice. To examine the tumorigenicity *in vivo*, the SP of MDA-MB-231 cells were inoculated into the mammary fat pad in nude

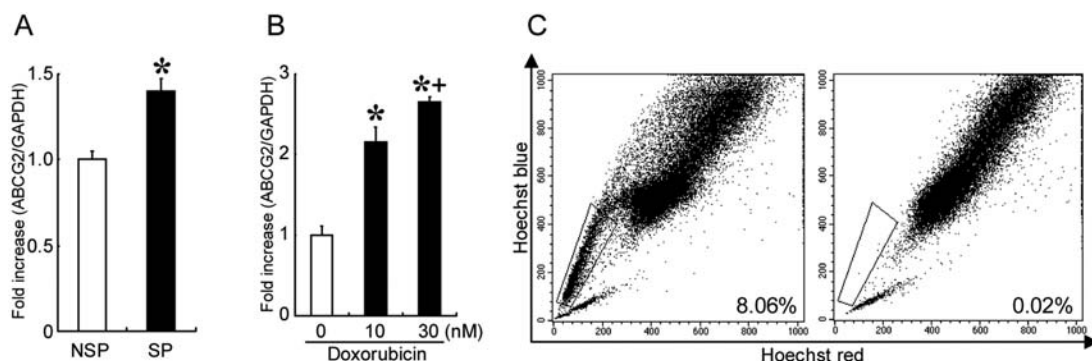


Figure 3. SP phenotype and ABCG2 expression. (A) Relative ABCG2 mRNA expression in SP and NSP of MDA-MB-231 cells determined by real-time RT-PCR. Data are shown as fold increase compared with NSP. *Significantly different from NSP ($p < 0.05$). (B) Relative ABCG2 mRNA expression in doxorubicin-resistant MDA-MB-231 cells determined by real-time RT-PCR. Data are shown as fold increase compared with doxorubicin-untreated (0 nM) control cells. *Significantly different from the control ($p < 0.05$), **significantly different from doxorubicin (10 nM) ($p < 0.05$). (C) Representative Hoechst 33342 dye staining profile of doxorubicin (10 nM)-resistant MDA-MB-231 cells in the absence (left) or presence of FTC (right). Percentages given in the lower right corner refer to the relative abundance of SP cells.

Inoculated cell no.	Tumor formation rate	
	NSP	SP
1,000	3/11	5/11
3,000	5/13	6/13

SP and NSP cells (1,000 or 3,000 cells/mouse) were inoculated into the mammary fat pad in nude mice (n=11 or 13). Tumor formation was assessed at 8 weeks after the cell inoculation.

mice. Tumor formation rates at 8 weeks after the cell inoculation were similar between SP and NSP cells (Table I). However, the tumor growth of SP cells was significantly accelerated compared with that of NSP cells (Fig. 5A).

The bone-metastatic potential of SP cells was next examined by inoculating the cells into the left cardiac ventricle in nude mice. Radiographic analysis demonstrated that both SP and NSP cells developed osteolytic bone metastases (Fig. 5B). The incidences of metastasis were similar between SP and NSP (NSP: 10/15, SP: 9/15, the number of mice with metastases/total mice). There was no significant difference in the lesion number and area (Fig. 5B, C).

SP abundance in bone metastases. We examined whether SP is increased in bone metastases by inoculating parental MDA-MB-231 cells into nude mice. The SP abundance in the tumor cells in bone metastases was comparable to that in the mammary tumors and in parental MDA-MB-231 cells in culture (Fig. 6).

Gene expression profile of SP cells. We finally performed a comprehensive analysis of gene expression differences between SP and NSP cells. The microarray data demon-

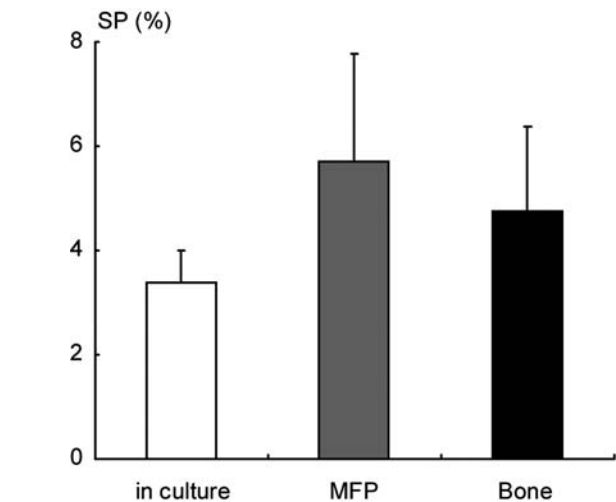


Figure 6. SP abundance in bone metastases of parental MDA-MB-231 cells. The abundance of SP (%) in tumor cells isolated from the tumors in mammary fat pad (MFP) and in bone (n=9/group) is shown. The SP abundance in parental MDA-MB-231 cells in culture is also shown as a control (left bar).

strated that 44 genes showed more than 1.5-fold up-regulation and 29 genes showed a >1.5-fold down-regulation (Table II). However, no up-regulation of known stem cell markers, potential cancer stem cell markers and metastasis-related genes was found in SP cells.

Discussion

Although several markers have been proposed to identify CSCs, the definitive markers have not been established in any types of CSC. In breast cancers, the cell surface markers CD24^{-low}/CD44⁺, high ALDH activity and SP are considered to be potential markers for CSCs (1,3-5,7). However, it is curious that the cell populations isolated using these markers do not always overlap (4). Consistent with these results, our data show that most MDA-MB-231 cells were CD24⁻/CD44⁺,

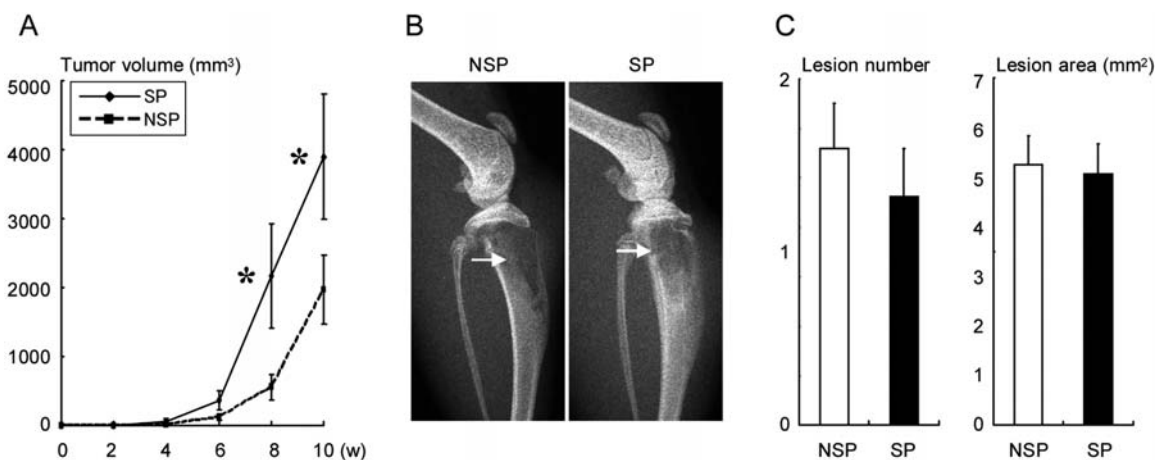


Figure 5. Tumorigenic and metastatic potential of the SP of MDA-MB-231 cells. (A) Tumor growth of SP and NSP cells (3,000 cells/mouse) in the orthotopic mammary fat pad in nude mice (n=6/group). *Significantly different from NSP (p<0.05). (B and C) Development of bone metastases in nude mice. SP and NSP cells (10,000 cells/mouse) were inoculated through the left cardiac ventricle (n=10/NSP, n=9/SP). (B) Representative radiographs of the osteolytic lesions in hindlimbs at 6 weeks after the cell inoculation (arrows, osteolytic bone metastases). (C) Six weeks after the cell inoculation, the lesion number (left) and area (right) of osteolytic bone metastases were measured on radiographs. Data are shown as lesion number/mouse or lesion area (mm²)/mouse.

Table II. Microarray analysis of the SP and NSP isolated from MDA-MB-231 cells.

Gene symbol	Gene description	Fold change	Status
MIPEP	Mitochondrial intermediate peptidase	2.66	Up
EIF4A2	Eukaryotic translation initiation factor 4A, isoform 2	2.5	Up
SNORA4	Small nucleolar RNA, H/ACA box 4	2.44	Up
TISP43	Similar to mCG22736	2.01	Up
FAM99A	Family with sequence similarity 99, member A	1.93	Up
KIR2DS5	Killer cell immunoglobulin-like receptor, two domains, short cytoplasmic tail, 5	1.93	Up
SNORD52	Small nucleolar RNA, C/D box 52	1.83	Up
SNORA1	Small nucleolar RNA, H/ACA box 1	1.79	Up
C15orf51	Chromosome 15 open reading frame 51	1.78	Up
LOC100130904	Similar to CD177 molecule	1.77	Up
IL28A	Interleukin 28A (interferon, λ 2)	1.74	Up
CXorf42	Chromosome X open reading frame 42	1.69	Up
LOC100132178	Similar to hCG2008275	1.69	Up
HIST2H2BE	Histone cluster 2, H2be	1.68	Up
LOC283588	NA	1.66	Up
LOC100129391	Similar to Zinc finger (CCCH type), RNA-binding motif and serine/arginine rich 2	1.65	Up
LOC100128830	NA	1.64	Up
FLJ31958	NA	1.63	Up
C3orf47	Chromosome 3 open reading frame 47	1.63	Up
WIF1	WNT inhibitory factor 1	1.63	Up
GAGE13	G antigen 13	1.62	Up
MIRN21	microRNA 21	1.62	Up
DEXI	Dexamethasone-induced transcript	1.62	Up
TAF12	NA	1.61	Up
MGC39584	Hypothetical gene supported by BC029568	1.59	Up
C4orf11	Chromosome 4 open reading frame 11	1.59	Up
FRMPD2	FERM and PDZ domain containing 2	1.59	Up
LOC100129420	Similar to hCG1990547	1.59	Up
OR4C13	Olfactory receptor, family 4, subfamily C, member 13	1.57	Up
SNORD75	Small nucleolar RNA, C/D box 75	1.56	Up
KCNIP1	Kv channel interacting protein 1	1.55	Up
LRMP	Lymphoid-restricted membrane protein	1.55	Up
C21orf94	Chromosome 21 open reading frame 94	1.54	Up
SNORA16B	Small nucleolar RNA, H/ACA box 16B	1.54	Up
ABCG2	ATP-binding cassette, sub-family G (WHITE), member 2	1.54	Up
TTC30B	Tetratricopeptide repeat domain 30B	1.53	Up
SNORD25	Small nucleolar RNA, C/D box 25	1.53	Up
FLJ30064	Hypothetical protein LOC644975	1.53	Up
HOXD10	Homeobox D10	1.53	Up
OR4D1	Olfactory receptor, family 4, subfamily D, member 1	1.52	Up
RP11-114H20.1	Hypothetical LOC401589	1.52	Up
C1orf62	Chromosome 1 open reading frame 62	1.52	Up
C4orf38	Chromosome 4 open reading frame 38	1.51	Up
SLFN12L	Schlafen family member 12-like	1.51	Up
OR4N4	Olfactory receptor, family 4, subfamily N, member 4	1.51	Up
HSPC072	NA	2.61	Down
C20orf69	Chromosome 20 open reading frame 69	2.05	Down
GABRE	γ -aminobutyric acid (GABA) A receptor, ϵ	1.99	Down

Gene symbol	Gene description	Fold change	Status
SLCO1B3	Solute carrier organic anion transporter family, member 1B3	1.93	Down
LOC221442	NA	1.88	Down
LCE2C	Late cornified envelope 2C	1.88	Down
CATSPER2P1	Cation channel, sperm associated 2 pseudogene 1	1.76	Down
LOC152118	NA	1.74	Down
SNORD41	Small nucleolar RNA, C/D box 41	1.74	Down
CDRT1	CMT1A duplicated region transcript 1	1.73	Down
LOC51336	Mesenchymal stem cell protein DSCD28	1.69	Down
ID2	Inhibitor of DNA binding 2, dominant negative helix-loop-helix protein	1.69	Down
LOC441233	Hypothetical gene supported by AK128010	1.68	Down
SNORA15	Small nucleolar RNA, H/ACA box 15	1.66	Down
FLJ27243	NA	1.64	Down
MMP1	Matrix metalloproteinase 1 (interstitial collagenase)	1.63	Down
DOC2B	Double C2-like domains, β	1.61	Down
OR7G1	Olfactory receptor, family 7, subfamily G, member 1	1.6	Down
OR1S1	Olfactory receptor, family 1, subfamily S, member 1	1.6	Down
SNORD38B	Small nucleolar RNA, C/D box 38B	1.59	Down
MARCH11	Membrane-associated ring finger (C3HC4) 11	1.59	Down
RBMV2EP	RNA binding motif protein, Y-linked, family 2, member E pseudogene	1.57	Down
N6AMT1	N-6 adenine-specific DNA methyltransferase 1 (putative)	1.54	Down
ENTPD3	Ectonucleoside triphosphate diphosphohydrolase 3	1.52	Down
KIR2DL3	Killer cell immunoglobulin-like receptor, two domains, long cytoplasmic tail, 3	1.52	Down
GOLGA6	Golgi autoantigen, golgin subfamily a, 6	1.52	Down
LOC646934	Similar to golgin-like protein	1.52	Down
LOC441956	Similar to cDNA sequence BC021523	1.51	Down
VCAN	Versican	1.51	Down

Up- (>1.5-fold) and down-regulated (>1.5-fold) genes in the SP of MDA-MB-231 cells are shown. NA, not applicable.

whereas a very small population of MDA-MB-231 cells possessed ALDH activity and a few percent of the cells entered the SP fraction. Extensive studies are awaited to determine the generalized markers for breast CSCs.

SP cells have been identified in a variety of human cancers and cancer cell lines and shown to have CSC-like properties (5,7). The SP of MDA-MB-231 cells also displayed CSC-like characteristics, such as enhanced tumor-sphere formation in culture and increased tumor growth in the mammary fat pad in nude mice. However, there are some reports indicating that SP does not completely define CSC-like cells (18,19). They demonstrated that, as well as SP cells, NSP cells gave rise to a significant proportion of SP cells. On the basis of stem cell physiology, SP cells should give rise to SP and NSP cells by means of asymmetric cell division, whereas NSP cells should not have this potential. In our study, the NSP of MDA-MB-231 cells also gave rise to SP, although the population was smaller than the SP generated from SP.

Furthermore, the NSP developed tumors in mammary fat pad in nude mice at a similar rate to the SP. These results collectively suggest that the SP of MDA-MB-231 cells possesses some of the CSC-like properties but does not completely meet the criteria for CSCs.

It has been suggested that the SP phenotype is conferred by the expression of ABC transporters, especially ABCB1 and ABCG2 (13,14). The SP fraction of MDA-MB-231 cells was eliminated in the presence of an ABCG2-specific inhibitor FTC. ABCG2 mRNA expression was significantly up-regulated in SP cells compared with that in NSP cells. These results suggest that ABCG2 is responsible, at least in part, for the SP phenotype of MDA-MB-231 cells.

CSCs are thought to be resistant to chemotherapy. One mechanism by which this may arise is through the expression of ABC transporters. In this respect, SP cells share similar properties with CSCs. The doxorubicin-resistant MDA-MB-231 cells exhibited higher ABCG2 expression and increased

SP fraction, suggesting a relationship between the SP phenotype and drug resistance. In contrast, these changes were not found in the 5-FU-resistant cells. Since ABC transporters responsible for the efflux of each chemotherapeutic agent are variable (17), it may be possible that 5-FU is effluxed by ABC transporters other than ABCB1 and ABCG2 in MDA-MB-231 cells.

The development of distant metastases is the major cause of death in patients with breast cancer. However, the role of CSCs in multistage cancer progression, particularly with respect to metastasis, has not been well defined. Breast cancer cells with CD24⁺/CD44⁺ subpopulation have been shown to have higher invasive properties (20). ALDH-positive populations of mammary carcinoma cell lines also display increased invasive characteristics (10). These findings suggest that CSCs possess higher metastatic potential. Furthermore, Balic *et al* have revealed an increase in CD24⁺/CD44⁺ cancer cells disseminated in bone marrow in breast cancer patients (21), suggesting that CSCs may have high metastatic potential to bone. Meanwhile, there are some reports showing that CSC phenotype alone is not enough to determine metastasis (1,20). Our results show that SP cells did not exhibit up-regulation of metastasis-related genes and did not cause increased metastases to bone. These results suggest that CSCs may not have higher metastatic potential to bone. Experiments using the definitive CSCs have to be performed to determine the role of CSCs in cancer metastasis.

We also found that the SP abundance in bone metastases in nude mice is comparable to those in mammary fat pad and in parental MDA-MB-231 cells in culture. However, the data do not exclude the possibility that SP cells may have a higher metastatic potential than NSP cells, because the results including ours indicate that the ratio of SP to NSP cells reached a steady state within a few weeks (22). Thus, it is possible that cancer cells initially metastasize as SP and then change their phenotype following limited differentiation at their new site.

It has been argued that the phenotypic differences between SP and NSP cells are a consequence of damage induced by the Hoechst dye, which is retained longer in NSP cells. Christgen *et al* proposed that the Hoechst dye directly affects the expression of stemness-related genes (23). In our study, monolayer cell proliferation was similar between SP and NSP. The expression of stem cell genes was also unaffected in NSP cells compared to that in SP cells. Thus, it is unlikely that the Hoechst dye directly caused the difference between SP and NSP in MDA-MB-231 cells, although it is difficult to exclude the possibility.

In conclusion, our results suggest that the SP of MDA-MB-231 cells possesses some of the properties of CSCs but does not have a higher metastatic potential to bone. However, since definite markers for CSCs have not been established yet, further studies are required to determine the bone metastatic potential of CSCs.

Acknowledgements

This study was supported by grants in aid from the Ministry of Education, Culture, Sports, Science and Technology, Japan (to T.H. and H.N.).

References

1. Visvader JE and Lindeman GJ: Cancer stem cells in solid tumours: accumulating evidence and unresolved questions. *Nat Rev Cancer* 8: 755-768, 2008.
2. Bonnet D and Dick JE: Human acute myeloid leukemia is organized as a hierarchy that originates from a primitive hematopoietic cell. *Nat Med* 3: 730-737, 1997.
3. Al-Hajj M, Wicha MS, Benito-Hernandez A, Morrison SJ and Clarke MF: Prospective identification of tumorigenic breast cancer cells. *Proc Natl Acad Sci USA* 100: 3983-3988, 2003.
4. Ginestier C, Hur MH, Charafe-Jauffret E, *et al.*: Aldh1 is a marker of normal and malignant human mammary stem cells and a predictor of poor clinical outcome. *Cell Stem Cell* 1: 555-567, 2007.
5. Wu C and Alman BA: Side population cells in human cancers. *Cancer Lett* 268: 1-9, 2008.
6. Goodell MA, Brose K, Paradis G, Conner AS and Mulligan RC: Isolation and functional properties of murine hematopoietic stem cells that are replicating in vivo. *J Exp Med* 183: 1797-1806, 1996.
7. Nakanishi T, Chumsri S, Khakpour N, *et al.*: Side-population cells in luminal-type breast cancer have tumour-initiating cell properties, and are regulated by HER2 expression and signalling. *Br J Cancer* 102: 815-826, 2010.
8. Mundy G: Metastasis to bone: causes, consequences and therapeutic opportunities. *Nat Rev Cancer* 2: 584-593, 2002.
9. Croker AK, Goodale D, Chu J, *et al.*: High aldehyde dehydrogenase and expression of cancer stem cell markers selects for breast cancer cells with enhanced malignant and metastatic ability. *J Cell Mol Med* 13: 2236-2252, 2008.
10. Charafe-Jauffret E, Ginestier C, Iovino F, *et al.*: Breast cancer cell lines contain functional cancer stem cells with metastatic capacity and a distinct molecular signature. *Cancer Res* 69: 1302-1313, 2009.
11. Hiraga T and Nakamura H: Imatinib mesylate suppresses bone metastases of breast cancer by inhibiting osteoclasts through the blockade of c-Fms signals. *Int J Cancer* 124: 215-222, 2009.
12. Hansford LM, McKee AE, Zhang L, *et al.*: Neuroblastoma cells isolated from bone marrow metastases contain a naturally enriched tumor-initiating cell. *Cancer Res* 67: 11234-11243, 2007.
13. Bunting KD, Zhou S, Lu T and Sorrentino BP: Enforced P-glycoprotein pump function in murine bone marrow cells results in expansion of side population stem cells in vitro and repopulating cells in vivo. *Blood* 96: 902-909, 2000.
14. Zhou S, Schuetz JD, Bunting KD, *et al.*: The ABC transporter Bcrp1/ABCG2 is expressed in a wide variety of stem cells and is a molecular determinant of the side-population phenotype. *Nat Med* 7: 1028-1034, 2001.
15. Rabindran SK, Ross DD, Doyle LA, Yang W and Greenberger LM: Fumitremorgin C reverses multidrug resistance in cells transfected with the breast cancer resistance protein. *Cancer Res* 60: 47-50, 2000.
16. Couture L, Nash JA and Turgeon J: The ATP-binding cassette transporters and their implication in drug disposition: a special look at the heart. *Pharmacol Rev* 58: 244-258, 2006.
17. Dean M: ABC transporters, drug resistance, and cancer stem cells. *J Mammary Gland Biol Neoplasia* 14: 3-9, 2009.
18. Lichtenauer UD, Shapiro I, Geiger K, *et al.*: Side population does not define stem cell-like cancer cells in the adrenocortical carcinoma cell line NCI H295R. *Endocrinology* 149: 1314-1322, 2008.
19. Mitsutake N, Iwao A, Nagai K, *et al.*: Characterization of side population in thyroid cancer cell lines: cancer stem-like cells are enriched partly but not exclusively. *Endocrinology* 148: 1797-1803, 2007.
20. Sheridan C, Kishimoto H, Fuchs RK, *et al.*: CD44⁺/CD24⁻ breast cancer cells exhibit enhanced invasive properties: an early step necessary for metastasis. *Breast Cancer Res* 8: R59, 2006.
21. Balic M, Lin H, Young L, *et al.*: Most early disseminated cancer cells detected in bone marrow of breast cancer patients have a putative breast cancer stem cell phenotype. *Clin Cancer Res* 12: 5615-5621, 2006.
22. Hirschmann-Jax C, Foster AE, Wulf GG, *et al.*: A distinct 'side population' of cells with high drug efflux capacity in human tumor cells. *Proc Natl Acad Sci USA* 101: 14228-14233, 2004.
23. Christgen M, Geffers R, Ballmaier M, *et al.*: Down-regulation of the fetal stem cell factor SOX17 by H33342: a mechanism responsible for differential gene expression in breast cancer side population cells. *J Biol Chem* 285: 6412-6418, 2010.